

Boundary of Quantum Evolution under Decoherence

Navin Khaneja ^{*}, Burkhard Luy, Steffen J. Glaser [†]

November 4, 2018

Abstract

Relaxation effects impose fundamental limitations on our ability to coherently control quantum mechanical phenomena. In this letter, we establish physical limits on how closely can a quantum mechanical system be steered to a desired target state in the presence of relaxation. In particular, we explicitly compute the maximum coherence or polarization that can be transferred between coupled nuclear spins in the presence of very general decoherence mechanisms that include cross-correlated relaxation. We give analytical expressions for the control laws (pulse sequences) which achieve these physical limits and provide supporting experimental evidence. Exploitation of cross-correlation effects has recently led to the development of powerful methods in NMR spectroscopy to study very large biomolecules in solution. We demonstrate with experiments that the optimal pulse sequences provide significant gains over these state of the art methods, opening new avenues for spectroscopy of much larger proteins. Surprisingly, in spite of very large relaxation rates, optimal control can transfer coherence without any loss when cross-correlated relaxation rates are tuned to auto-correlated relaxation rates.

^{*}To whom correspondence may be addressed. Division of Applied Sciences, Harvard University, Cambridge, MA 02138. Email:navin@hrl.harvard.edu

[†]Institute of Organic Chemistry and Biochemistry II, Technische Universität München, 85747 Garching, Germany. This work was funded by the Fonds der Chemischen Industrie and the Deutsche Forschungsgemeinschaft under grant Gl 203/4-1.

1 Introduction

The control of quantum ensembles has many applications, ranging from coherent spectroscopy to quantum information processing. In practice, the quantum system of interest is not isolated but interacts with its environment. This leads to the phenomenon of relaxation, which results in signal loss and ultimately limits the range of applications. Relaxation is a major road block standing in the way of practical quantum computing. Manipulating quantum systems in a manner that minimizes relaxation losses is a fundamental challenge of utmost practical importance. What is the ultimate limit on how close an ensemble of quantum systems can be steered from an initial state to a desired target state in the presence of relaxation? Until now there existed no theory that answers this question. This situation is comparable to the time before the fundamental limits of a heat engine were known: More than hundred years after the invention of the steam engine, the physical limits for the maximum amount of work a steam engine could produce was unclear, in spite of decades of advances in its design. "The theory of its operation is rudimentary and attempts to improve its performance are still made in an almost haphazard way" [1]. Of course, the maximum efficiency of a heat engine is not given by the cleverness of the engineer who attempts to build such a machine, but by the fundamental law of thermodynamics as captured in Carnot's principle.

In this manuscript we derive fundamental limits on how close can an ensemble of nuclear spins be driven from its initial state to a desired target state in the presence of relaxation. In particular, we derive the maximum efficiency of polarization and coherence transfer between coupled nuclear spins. A premier example where such coherence transfer operations are important is nuclear magnetic resonance (NMR) spectroscopy [2]. In structural biology, NMR spectroscopy is an important technique that allows to determine the structure of biological macro molecules, such as proteins, in aqueous solution. With increasing size of molecules or molecular complexes, the rotational tumbling of the molecules becomes slower and leads to increased relaxation losses. When these relaxation rates become comparable to the spin-spin couplings, the efficiency of coherence transfer is considerably reduced, leading to poor sensitivity and increased measurement times. Recent advances have made it possible to significantly extend the size limit of biological macro molecules amenable to study by liquid state NMR [3-6]. These techniques take advantage of the phenomenon of cross-correlated relaxation. Cross-correlated relaxation represents interference effects between two different relaxation mechanisms [8]. Until now it was not clear if further improvements can be made and what is the physical limit for the coherence transfer efficiency between coupled spins in the presence of

cross-correlated relaxation.

In this letter, we give analytical expressions for this maximum achievable coherence transfer efficiency for two heteronuclear coupled spins under very general decoherence mechanisms that include cross-correlated relaxation. We describe the optimal pulse sequences that achieve this efficiency and experimental data that supports these results. We demonstrate that in the limit where the interference effects become comparable to the uncorrelated relaxation rates, complete coherence transfer is possible without any loss. In the general case of cross-correlated relaxation, we demonstrate substantial improvement over previously known sequences in NMR spectroscopy.

2 Theory

We consider an isolated heteronuclear spin system consisting of two coupled spins 1/2, denoted I (e.g. ^1H) and S (e.g. ^{15}N). To fix ideas, we first address the problem of selective population inversion of two energy levels (e.g. $\alpha\beta$ and $\beta\beta$) as shown in Fig. 1. This is a central step in high-resolution multi-dimensional NMR spectroscopy and corresponds to the transfer of an initial density operator I_z , representing polarization on spin I , to the target state $2I_zS_z$.

For large molecules in the so-called spin diffusion limit [2], where longitudinal relaxation rates are negligible compared to transverse relaxation rates, both the initial term (I_z) and final term ($2I_zS_z$) of the density operator are long-lived. However, the transfer between these two states requires the creation of coherences which in general are subject to transverse relaxation. The two principle transverse relaxation mechanisms are dipole-dipole (DD) relaxation and relaxation due to the chemical shift anisotropy (CSA) of spins I and S . The quantum mechanical equation of motion (Liouville-von Neumann equation) for the density operator ρ [2] is given by

$$\begin{aligned} \dot{\rho} = & \pi J[-i2I_zS_z, \rho] + \pi k_{DD}[2I_zS_z, [2I_zS_z, \rho]] + \pi k_{CSA}^I[I_z, [I_z, \rho]] + \pi k_{CSA}^S[S_z, [S_z, \rho]] \\ & + \pi k_{DD/CSA}^I[2I_zS_z, [I_z, \rho]] + \pi k_{DD/CSA}^S[2I_zS_z, [S_z, \rho]], \end{aligned} \quad (1)$$

where J is the heteronuclear coupling constant. The rates k_{DD} , k_{CSA}^I , k_{CSA}^S represent auto-relaxation rates due to DD relaxation, CSA relaxation of spin I and CSA relaxation of spin S , respectively. The rates $k_{DD/CSA}^I$ and $k_{DD/CSA}^S$ represent cross-correlation rates of spin I and S

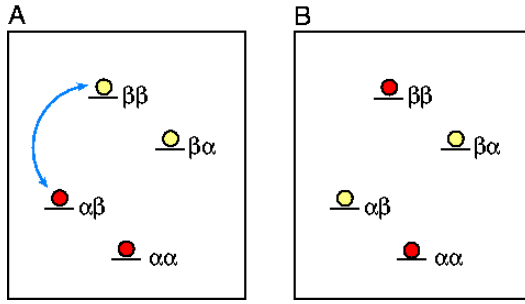


Figure 1: Selective population inversion of the energy levels $\alpha\beta$ and $\beta\beta$, corresponding to a transfer of polarization I_z (A) to $2I_z S_z$ (B).

caused by interference effects between DD and CSA relaxation. These relaxation rates depend on various physical parameters, such as the gyromagnetic ratios of the spins, the internuclear distance, the CSA tensors, the strength of the magnetic field and the correlation time of the molecular tumbling [2]. Let the initial density operator $\rho(0) = A$ and $\rho(t)$ denote the density operator at time t . The maximum efficiency of transfer between A and target operator C is defined as the largest possible value of $\text{trace}(C^\dagger \rho(t))$ for any time t [3] (by convention operators A and C are normalized).

The main result of this letter is as follows. The maximum efficiency of transfer between the operators I_z and $2I_z S_z$ depends only on the scalar coupling constant J and the net auto-correlated and cross-correlated relaxation rates of spin I , given by $k_a = k_{DD} + k_{CSA}^I$ and $k_c = k_{DD/C}^I$, respectively. This physical limit η is given by

$$\eta = \sqrt{1 + \zeta^2} - \zeta, \quad (2)$$

where

$$\zeta = \sqrt{\frac{k_a^2 - k_c^2}{J^2 + k_c^2}}. \quad (3)$$

The derivation of the maximum efficiency rests on the basic principles of optimal control theory and the development of a new class of control systems (see suppl. material for details). The optimal transfer scheme (CROP: cross-correlated relaxation optimized pulse) has two constants of motion. If $l_1(t)$ and $l_2(t)$ denote the two-dimensional vectors $(\langle I_x \rangle(t), \langle I_y \rangle(t))$ and $(\langle 2I_x S_z \rangle(t), \langle 2I_y S_z \rangle(t))$, respectively, then throughout the transfer process the ratio of the magnitudes of the vectors l_2 and l_1 is maintained constant at η . Furthermore, the angle γ^* between l_1 and l_2 is constant throughout. The two constants of motion of the optimal transfer scheme determine the amplitude and phase of the rf field at each point in time and explicit expressions for the optimal pulse sequence can be derived (see suppl. material).

We now consider two important limiting cases of this problem:

(I) In the case when $k_a > 0$ and $k_c = 0$ (no cross-correlated relaxation), the optimal efficiency η is equal to $\sqrt{1 + \frac{k_a^2}{J^2}} - \frac{k_a}{J} < 1$ (see yellow curves in Figs. 2 and 3) and the optimal angle γ^* is $\pi/2$ [9].

(II) In the limit where the cross-correlation coefficient k_c/k_a approaches 1, the optimal transfer efficiency η approaches 1 (see black curves in Figs. 2 and 3) and γ^* approaches π . Surprisingly, in this case using optimal control it is possible to transfer coherence without any loss in the presence of relaxation. In the limit of large relaxation rates k_a , this relaxation-optimized transfer mechanism gains up to 100% compared to state of the art transfer schemes.

The optimal transfer scheme is best illustrated by decomposing the initial operator I_z as a sum of the two operators $I_z S_\alpha = \frac{I_z}{2} + I_z S_z$ and $I_z S_\beta = \frac{I_z}{2} - I_z S_z$. The transverse components $I_x S_\alpha$, $I_y S_\alpha$ and $I_x S_\beta$, $I_y S_\beta$ relax with rates $k_a + k_c$ and $k_a - k_c$, respectively. When k_c/k_a approaches 1, the transverse operators $I_x S_\beta$ and $I_y S_\beta$ do not relax. The optimal control in this case reduces to selectively inverting $I_z S_\beta$ to $-I_z S_\beta$ by weak rf irradiation at the frequency $(-J/2)$ of the slowly relaxing multiplet component. Such selective inversions have been performed in the past in the absence of cross-correlated relaxation [10, 11]. However, since the component $I_z S_\alpha$, which we do not want to invert, has a large transverse relaxation rate given by $k_a + k_c$, it is possible to carry out the

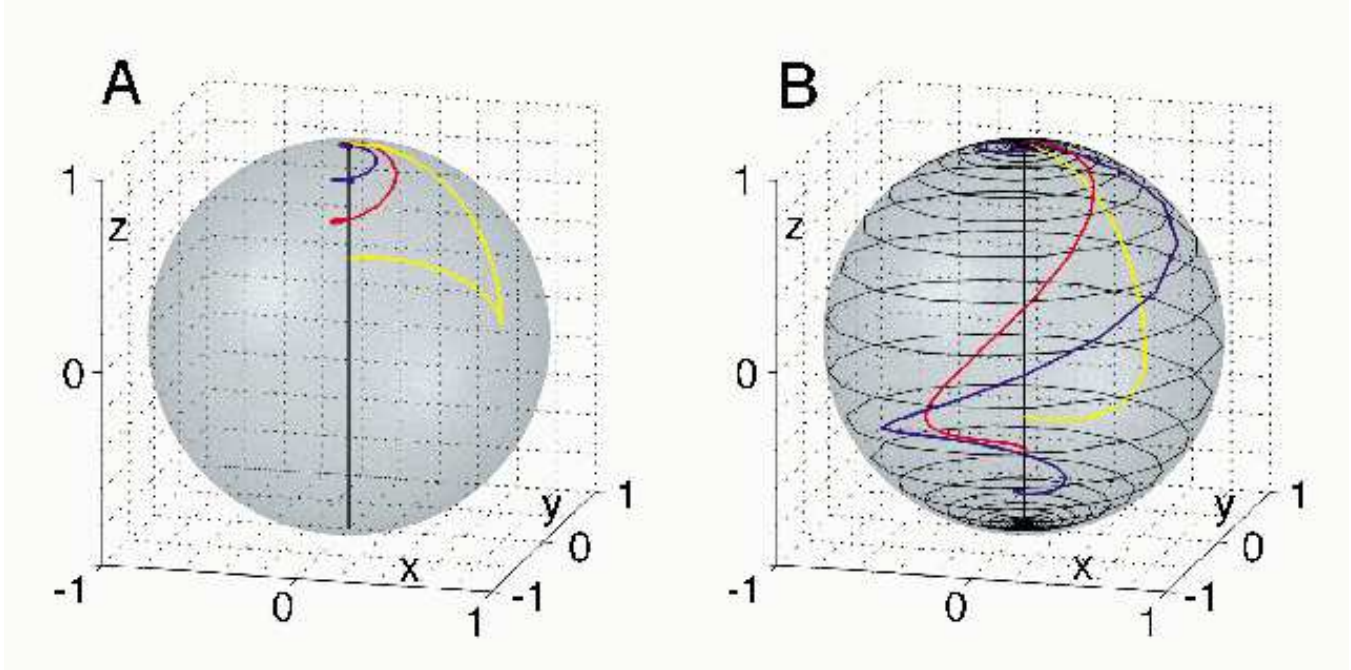


Figure 2: Optimal trajectories of the two multiplet components (A) $\vec{I}S_\alpha$ and (B) $\vec{I}S_\beta$ for $k_a = J$ and $k_c/k_a = 0$ (yellow curves), $k_c/k_a = 0.75$ (red curves), $k_c/k_a = 0.95$ (blue curves), $k_c/k_a = 0.999$ (black curve).

selective inversion process much more rapidly. In Fig. 2, optimal trajectories of the two multiplet components are shown for several cross-correlation coefficients k_c/k_a and $k_a = J$.

In Fig. 4, the optimal rf amplitude and irradiation frequency of a CROP sequence is shown as a function of time for the case $k_c/k_a = 0.75$ and $k_a = J$. Although the ideal sequence has a long duration, most of the transfer occurs in a relatively short time window, outside of which the rf amplitude is vanishingly small. The transfer efficiency η is shown in Fig. 3 A for several ratios k_c/k_a as a function of the auto-correlated relaxation rate k_a/J . For the case $k_c/k_a = 0.75$, the physical limit of the transfer efficiency is compared in Fig. 3 B to the transfer efficiency of conventional transfer schemes.

The optimal control methods for the transfer from I_z to $2I_zS_z$ in the presence of cross-correlated relaxation immediately extend to other routinely used transfer, such as inphase to inphase transfer ($I_x \rightarrow S_x$) [12] and single transition to single transition transfer ($2I_xS^\alpha \rightarrow 2I^\alpha S_x$) [4]. Since the operators I_z , S_z and $2I_zS_z$ do not decay, the optimal efficiency for the transfer I_x to S_x is achieved by first rotating I_x to I_z (which can be done rapidly with negligible loss). Then I_z is transferred optimally to $2I_zS_z$ with efficiency η (Eq. 2), followed by the optimal transfer of $2I_zS_z$ to S_z , which is

finally rotated rapidly to S_x . The optimal transfer $2I_z S_z \rightarrow S_z$ is analogous to the optimal transfer $I_z \rightarrow 2I_z S_z$. The efficiency η' for this transfer is also given by Eq. (2), where the rates k_a and k_c are replaced by the corresponding rates $k'_a = k_{DD} + k_{CSA}^S$ and $k'_c = k_{DD/CSA}^S$ for spin S and ζ is replaced by the corresponding ζ' . The maximum efficiency for the transfer $I_x \rightarrow S_z$ is the product of the efficiencies of the individual steps (see Table 1).

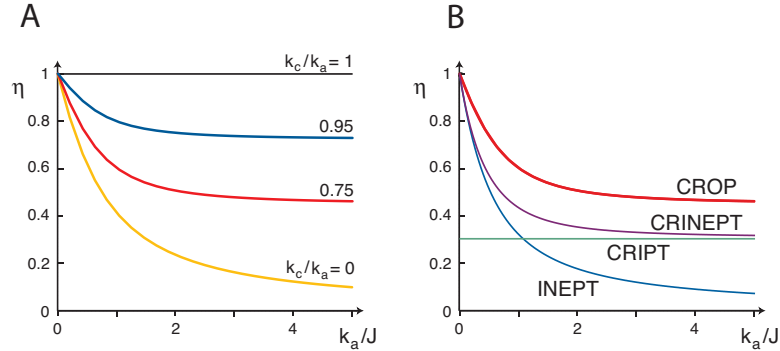


Figure 3: (A) Physical limits of the transfer efficiency η as a function of k_a/J for $k_c/k_a = 0$ (yellow curve), $k_c/k_a = 0.75$ (red curve), $k_c/k_a = 0.95$ (blue curve), $k_c/k_a = 1$ (black curve). (B) For the case $k_c/k_a = 0.75$, the theoretical bound of the transfer efficiency (CROP: red curve) is compared to the transfer efficiency of conventional transfer schemes (INEPT: blue curve, CRIPT: green curve, CRINEPT: purple curve).

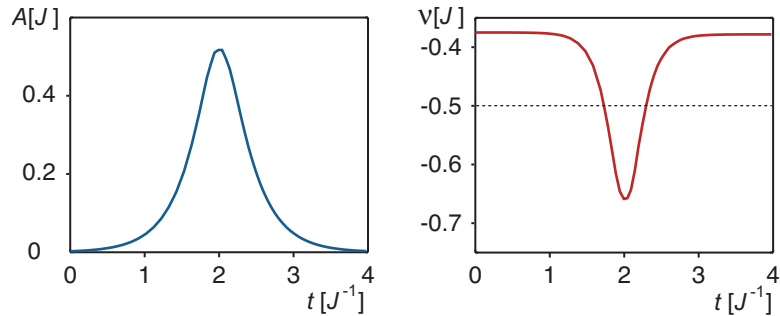


Figure 4: Truncated cross-correlated relaxation optimized pulse (CROP) for $k_c/k_a = 0.75$ and $k_a = J$: Radio frequency amplitude $A = \gamma B_0/2\pi$ (left) and irradiation frequency ν (right) as a function of time.

In the light of increasing use and superiority of TROSY (Transverse Relaxation-Optimized Spectroscopy) methods [4], the single transition to single transition transfer $2I_x S^\alpha \rightarrow 2I^\alpha S_x$ is important in NMR applications to structural biology. It is of both theoretical and practical interest to establish the physical limits for this transfer. This transfer can be achieved optimally as a sequence of the following steps. First the term $2I_x S^\alpha$ is rapidly rotated to $2I_z S^\alpha = I_z + 2I_z S_z$. In a second step,

Table 1: Bounds on Coherence and Polarization Transfer

Transfer	Physical Limits of Efficiency
$I_z \leftrightarrow 2I_z S_z$	$\eta = \sqrt{1 + \zeta^2} - \zeta$
$2I_z S_z \leftrightarrow S_z$	$\eta' = \sqrt{1 + \zeta'^2} - \zeta'$
$I_z \leftrightarrow S_z$	$\frac{\eta\eta'}{\sqrt{\eta^2 + \eta'^2}}$
$I_x S_\alpha \leftrightarrow I_\alpha S_x$	$\sqrt{\eta^2 + \eta'^2}$

$2I_z S_z$ is transferred via CROP to S_z , followed by the CROP transfer of I_z to $2I_z S_z$. This completes the transfer from $2I_x S^\alpha$ to $2I^\alpha S_z$ which is finally rapidly rotated to $2I^\alpha S_x$. The maximum overall transfer efficiency is given by $\sqrt{\eta^2 + \eta'^2}$ (c.f. Table 1).

3 Experimental results

The performance of the analytically derived CROP sequences was tested experimentally using the coupled two-spin system of ^{13}C -labeled sodium formate with a coupling of $J = 193.6$ Hz between the ^{13}C spin (denoted I) and the ^1H spin (denoted S). In order to control the rotational correlation time, sodium formate was dissolved in a mixture of 96% D_6 -glycerol and 4% D_2O . The viscosity of this solvent can be conveniently adjusted through a variation of temperature. The experiments were performed at a temperature of 256.5 K where $k_a/J \approx 1$ (see Fig. 5 A) and 260 K where $k_a/J \approx 0.5$ (see Fig. 5 B). At a magnetic field of 17.6 T, the experimentally determined ratio of cross and auto correlation rate was $k_c/k_a \approx 0.75$. In the preparation phase of the experiments, the thermal equilibrium ^1H magnetization was dephased by applying a 90° proton pulse followed by a pulsed magnetic field gradient. The transfer efficiency of ^{13}C polarization I_z to $2I_z S_z$ was measured for the novel CROP sequence, as well as for INEPT [13], CRIPT [14] and CRINEPT [7] sequences. Finally, a hard 90_y° proton pulse was applied to transform $2I_z S_z$ to $2I_z S_x$ and the amplitude of the resulting proton anti-phase signal was measured. The resulting experimental transfer amplitudes are shown in Fig. 5 as a function of the transfer time. CROP sequences were truncated symmetrically to acquire transfer amplitudes also for finite mixing times. Experimentally, the optimal transfer time of the CROP sequence was found to be 7.5 ms. This is a compromise between losses due to the truncation of the (very long) CROP sequence and losses due to the non-zero relaxation rates of the terms $I_z S_z$. The experimentally determined relaxation time of these terms was about 50 ms. In spite of these non-idealities of the model system, the CROP sequences are substantially more efficient than the conventional sequences. In Fig. 5 A and B, the experimental gains compared to CRINEPT are 34%

and 22%, respectively. We found that although the optimal pulse sequences were designed for specific rates k_a and k_c , they were robust to variations in these parameters.

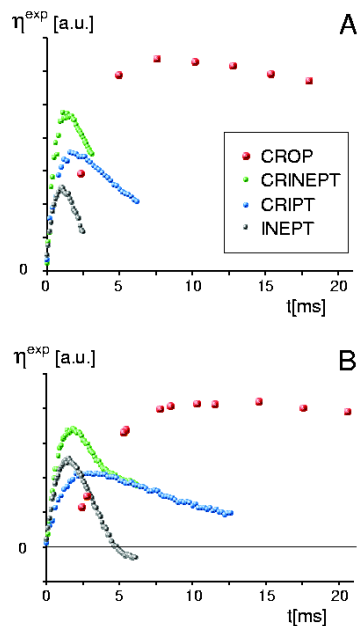


Figure 5: Experimental transfer amplitude of truncated CROP sequences compared to CRINEPT, CRIPT, and INEPT as a function of total transfer time. The experiments were performed at a temperature of 256.5 K with $k_a/k_c \approx 1.1$ (A) and 260 K with $k_a/k_c \approx 0.6$ (B).

4 Conclusion

Here, we derived for the first time upper achievable physical limits on the efficiency of coherence and polarization transfer for two coupled spins in the presence of very general decoherence mechanisms that include cross-correlated relaxation. In this letter, the focus was on the study of polarization and coherence transfer between an isolated pair of scalar coupled heteronuclear spins in the spin diffusion limit. For this example, new transfer schemes were found which yield substantial gains (of up to 100%) in transfer efficiency over conventional methods. With these physical limits established, it is expected that significant improvement can be achieved over state of the art experiments in protein NMR spectroscopy. Work is in progress to incorporate practical considerations like broadbandness and robustness with respect to variations of relaxation rates and experimental imperfections. The

methods presented here can be generalized for finding relaxation optimized pulse sequences in larger spin systems as commonly encountered e.g. in backbone and side chain assignments in protein NMR spectroscopy. Furthermore these methods directly extend to other routinely used experiments like excitation of multiple quantum coherence [2]. The most surprising aspect of the presented results is that in spite of large relaxation rates, it is possible to exploit the structure of relaxation and have decoherence-free evolution by steering the system through a decoherence-free subspace. It is also expected that the methods presented here will be further developed to minimize decoherence losses in various proposed implementations of quantum information processing.

References

- [1] S. Carnot, "Réflexions sur la puissance motrice du feu", (1824); "Reflections on the Motive Power of Fire", trans. Robert Fox (New York: Lilian Barber Press, 1986).
- [2] R. R. Ernst, G. Bodenhausen, A. Wokaun, *Principles of Nuclear Magnetic Resonance in One and Two Dimensions*, (Clarendon Press, Oxford, 1987).
- [3] S. J. Glaser, T. Schulte-Herbrüggen, M. Sieveking, O. Schedletsky, N. C. Nielsen, O. W. Sørensen, C. Griesinger, *Science*. **208**, 421 (1998).
- [4] K. Pervushin, R. Riek, G. Wider, K. Wüthrich, *Proc. Natl. Acad. Sci. USA* **94**, 12366 (1997).
- [5] M. Salzmann, K. Pervushin, G. Wider, H. Senn, K. Wüthrich, *Proc. Natl. Acad. Sci. USA* **95**, 13585 (1998).
- [6] K. Wüthrich, *Nat. Struct. Biol.* **5**, 492 (1998).
- [7] R. Riek, G. Wider, K. Pervushin, K. Wüthrich, *Proc. Natl. Acad. Sci. USA* **96**, 4918 (1999).
- [8] M. Goldman, *J. Magn. Reson.* **60**, 437 (1984).
- [9] N. Khaneja, T. Reiss, B. Luy, S. J. Glaser, quant-ph/0208050 (2002).
- [10] R. A. Hoffman, S. Forsén, *Progr. NMR Spectrosc.* **1**, 34, Pergamon Press, Oxford (1966).
- [11] K. G. R. Pachler, P. L. Wessels, *J. Magn. Reson.* **12**, 337 (1973).
- [12] D. P. Burum, R. R. Ernst, *J. Magn. Reson.* **39**, 163 (1980).
- [13] G. A. Morris, R. Freeman, *J. Am. Chem. Soc.* **101**, 760 (1979).

[14] R. Brüschweiler, R. R. Ernst, *Chem. Phys.* **96**, 1758 (1992).

5 Supplementary Material: Derivation of Optimal Control of Coherence Transfer under Cross-Correlated Relaxation

The derivation of optimal control assumes that the two heteronuclear spins have well separated resonance frequencies, allowing for fast selective manipulation of each spin on a time-scale determined by the coupling J and the relaxation rates k_a and k_c . Therefore the Cartesian spin operator I_z can be transformed to an operator of the form $I_x \cos \beta_1 + I_z \sin \beta_1$ by the use of strong, spin-selective radio frequency (rf) pulses without relaxation losses (see Fig. 6). Let $r_1(t)$ represent the magnitude of polarization and in-phase coherence on spin I at any given time t , i.e. $r_1^2(t) = \langle I_x \rangle^2 + \langle I_y \rangle^2 + \langle I_z \rangle^2$ (where e.g. $\langle I_x \rangle = \text{trace}\{\rho I_x\}$ represents the expectation value of I_x). Let $l_1(t)$ be the magnitude of in-phase coherence on spin I , i.e. $l_1^2(t) = \langle I_x \rangle^2 + \langle I_y \rangle^2$ and $\beta_1 = \cos^{-1} \frac{l_1}{r_1}$ (see Fig. 6). Using rf fields, we can exactly control the angle β_1 . Hence we can think of $\cos \beta_1$ as a control parameter and denote it by u_1 (see Fig. 6). Observe that the operator I_z is invariant under the evolution equation (1), whereas I_x and I_y evolve under the J coupling and also relax. For example, I_x evolves under the coupling to $2I_y S_z$ with rate J and cross relaxes to $-2I_x S_z$ with rate k_c . In the plane defined by the operators $2I_x S_z$ and $2I_y S_z$, the direction in which antiphase coherence begins to build up from an initial coherence I_x forms an angle

$$\theta = \tan^{-1}\left(\frac{J}{-k_c}\right)$$

with the axis $2I_x S_z$.

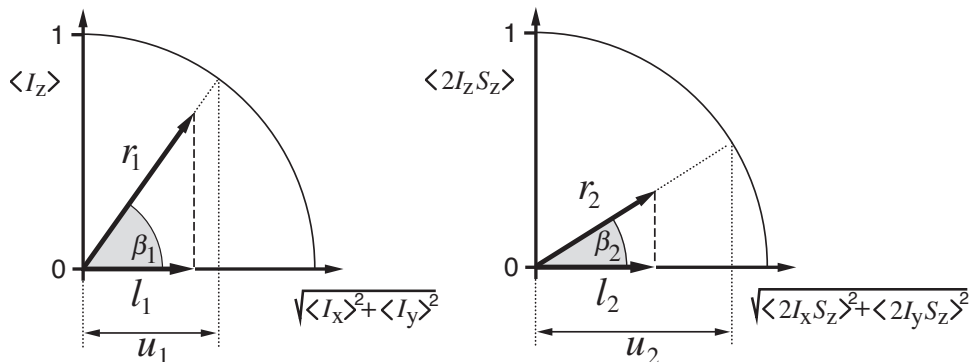


Figure 6: Representation of the system variables r_1 , r_2 , their transverse components l_1 , l_2 , the angles β_1 , β_2 , and of the control parameters $u_1 = \cos \beta_1$, $u_2 = \cos \beta_2$ in terms of the expectation values $\langle I_x \rangle$, $\langle I_y \rangle$, $\langle I_z \rangle$, $\langle 2I_x S_z \rangle$, $\langle 2I_y S_z \rangle$, and $\langle 2I_z S_z \rangle$.

As the operators $2I_xS_z$ and $2I_yS_z$ are produced, they also relax. Let $l_2(t)$ measure the magnitude of the total antiphase coherence at time t , i.e. $l_2^2(t) = \langle 2I_xS_z \rangle^2 + \langle 2I_yS_z \rangle^2$. By use of rf pulses it is possible to rotate the antiphase operators $2I_xS_z$ and $2I_yS_z$ to $2I_zS_z$, which is protected from relaxation. Let r_2 represent the total magnitude of the expectation values of these bilinear operators, i.e. $r_2^2(t) = l_2^2 + \langle 2I_zS_z \rangle^2$ and $\beta_2 = \cos^{-1} \frac{l_2}{r_2}$ (see Fig. 6). We can control the angle β_2 and we define $\cos \beta_2$ as a second control parameter u_2 (see Fig. 6).

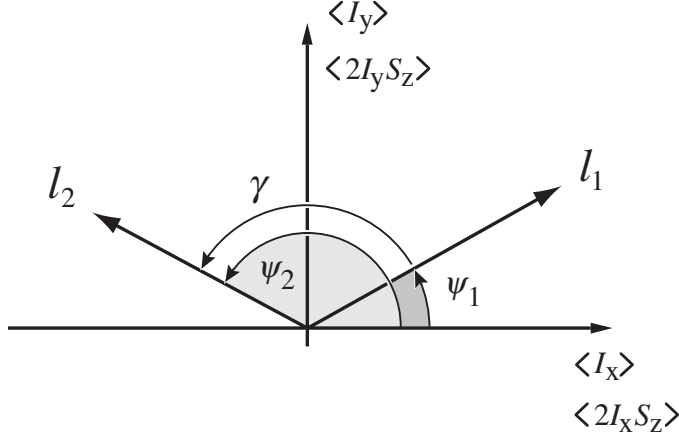


Figure 7: The figure shows the transverse planes defined by I_x and I_y superimposed on the plane defined by $2I_xS_z$ and $2I_yS_z$ such that I_x is aligned with $2I_xS_z$. l_1 and l_2 are the vectors representing transverse coherences in these two planes and γ is the angle between the vectors.

We superimpose the transverse planes defined by I_x and I_y with the plane defined by $2I_xS_z$ and $2I_yS_z$ such that I_x is aligned with $2I_xS_z$ (see Fig. 7). If γ represents the angle between l_1 and l_2 , then by definition of θ we have

$$\begin{aligned} \frac{d}{dt} l_1(t) &= -\pi [k_a l_1(t) - \sqrt{k_c^2 + J^2} \cos(\theta + \gamma) l_2(t)] \\ \frac{d}{dt} l_2(t) &= -\pi [k_a l_2(t) - \sqrt{k_c^2 + J^2} \cos(\theta - \gamma) l_1(t)]. \end{aligned}$$

This can be rewritten as

$$\frac{d}{dt} \begin{bmatrix} l_1(t) \\ l_2(t) \end{bmatrix} = \pi J \begin{bmatrix} -\xi & \chi \cos(\theta + \gamma) \\ \chi \cos(\theta - \gamma) & -\xi \end{bmatrix} \begin{bmatrix} l_1(t) \\ l_2(t) \end{bmatrix}, \quad (4)$$

where

$$\xi = k_a/J$$

and

$$\chi = \sqrt{1 + \left(\frac{k_c}{J}\right)^2}.$$

For a given value of β_1 and β_2 , we have $l_1(t) = r_1(t) \cos(\beta_1)$ and $l_2(t) = r_2(t) \cos(\beta_2)$. Since $\frac{d\langle I_z \rangle}{dt} = 0$ and $\frac{d\langle 2I_z S_z \rangle}{dt} = 0$, we get $\dot{r}_1(t) = \dot{l}_1(t) \cos(\beta_1)$ and $\dot{r}_2(t) = \dot{l}_2(t) \cos(\beta_2)$. Substituting for \dot{l}_1 and \dot{l}_2 , we then get

$$\frac{d}{dt} \begin{bmatrix} r_1(t) \\ r_2(t) \end{bmatrix} = \pi J \begin{bmatrix} -\xi u_1^2 & \chi u_1 u_2 \cos(\theta + \gamma) \\ \chi u_1 u_2 \cos(\theta - \gamma) & -\xi u_2^2 \end{bmatrix} \begin{bmatrix} r_1(t) \\ r_2(t) \end{bmatrix}. \quad (5)$$

Given the dynamical system in equation (5), we want to find the optimal values of $u_1(t)$, $u_2(t)$, and $\gamma(t)$, so that starting from $r_1(0) = 1$ we achieve the largest value for r_2 .

As the operator I_z is transferred to $2I_z S_z$, the ratio $\frac{r_2}{r_1}$ increases from 0 to ∞ . The optimal choice of u_1 and u_2 must ensure that the ratio of gain dr_2 in r_2 to loss dr_1 in r_1 for incremental time steps dt is maximized at each step. This ratio is

$$\frac{|\dot{r}_2|}{|\dot{r}_1|} = \frac{-\xi u_2^2 r_2 + \chi u_1 u_2 r_1 \cos(\theta - \gamma)}{\xi u_1^2 r_1 - \chi u_1 u_2 \cos(\theta + \gamma) r_2}.$$

Let $\frac{u_2 r_2}{u_1 r_1} = g$, then the above expression can be re-written as

$$\frac{|\dot{r}_2|}{|\dot{r}_1|} = \frac{r_1}{r_2} \frac{-\xi g^2 + \chi g \cos(\theta - \gamma)}{\xi - \chi g \cos(\theta + \gamma)}.$$

This expression needs to be maximized with respect to choice of g and γ . Let these optimal values be η and γ^* respectively. Then

$$\frac{d}{dg} \left. \frac{|\dot{r}_2|}{|\dot{r}_1|} \right|_{g=\eta, \gamma=\gamma^*} = 0$$

yields

$$\frac{1}{\eta} \cos(\theta - \gamma^*) + \eta \cos(\theta + \gamma^*) = \frac{2\xi}{\chi}, \quad (6)$$

which yields $\frac{|\dot{r}_2|}{|\dot{r}_1|} = \frac{r_1}{r_2} \eta^2$. Now the value of γ^* in equation (6) is such that it maximizes η . Differentiating both sides of equation (6) with respect to γ^* and substituting $\frac{d\eta}{d\gamma^*} = 0$, we obtain that

$$\frac{1}{\eta} \sin(\theta - \gamma^*) - \eta \sin(\theta + \gamma^*) = 0. \quad (7)$$

The optimal η and γ^* then satisfy equations (6, 7). The two equations can then be solved to give

$$\eta = \sqrt{\zeta^2 + 1} - \zeta, \quad (8)$$

where $\zeta = \sqrt{\frac{k_g^2 - k_c^2}{J^2 + k_c^2}}$ and optimal $\gamma^* = \tan^{-1} \frac{1 - \eta^2}{(1 + \eta^2) \cot \theta}$. By substituting the optimal control law $\frac{u_2(t)}{u_1(t)} = \frac{\eta r_1(t)}{r_2(t)}$, and integrating equation (5), we see that r_2 increases from 0 to $\sqrt{\zeta^2 + 1} - \zeta$, which is then the maximum achievable transfer.

We see that throughout the optimal transfer, the angle γ is maintained constant at γ^* . The optimal control ensures that the ratio of the transverse components $l_2(t)$ and $l_1(t)$ is always maintained constant at η . These two constraints can now be used to get explicit expressions for the magnitude and phase of the optimal rf-field.

Let ϕ denote the phase of the rf-field relative to l_1 ($\gamma - \phi$ relative to l_2) and let A be its amplitude. Let dl_1^\perp denote the change in transverse component perpendicular to the vector l_1 by application of the rf field in small time dt . Then observe $dl_1^\perp = 2\pi A \langle I_z \rangle \cos(\phi) dt$. Similarly $dl_2^\perp = 2\pi A \langle 2I_z S_z \rangle \cos(\gamma - \phi) dt$. If $\frac{l_2}{l_1}$ is maintained at η then the angle γ does not change due to the evolution equation (4). Therefore we only need to consider the change in γ , due to the rf field. If γ is maintained constant, then $\frac{dl_1^\perp}{l_1} = \frac{dl_2^\perp}{l_2}$. This gives $\tan(\beta_1) \cos(\phi) = \tan(\beta_2) \cos(\gamma^* - \phi)$ because $\frac{\langle I_z \rangle}{l_1} = \tan \beta_1$ and $\frac{\langle 2I_z S_z \rangle}{l_2} = \tan \beta_2$. This then implies that

$$\phi = \tan^{-1} \left(\frac{\tan \beta_1}{\tan \beta_2 \sin \gamma^*} - \cot \gamma^* \right).$$

The amplitude can be determined from the condition that $\frac{l_2(t)}{l_1(t)}$ is maintained constant. This implies that $\frac{dl_1}{l_1} = \frac{dl_2}{l_2}$. Substituting $dl_1 = (-\xi\pi J l_1 - \chi\pi J \cos(\theta + \gamma) l_2 + 2\pi A \langle I_z \rangle \sin(\phi)) dt$ and $dl_2 = (-\xi\pi J l_2 - \chi\pi J \cos(\theta - \gamma) l_1 - 2\pi A \langle 2I_z S_z \rangle \sin(\gamma - \phi)) dt$, we get

$$A = \frac{1}{2\pi} \frac{(\cos(\theta - \gamma^*) - \eta^2 \cos(\theta + \gamma^*)) \chi J}{(\tan \beta_1 \sin \phi + \tan \beta_2 \sin(\gamma^* - \phi)) \eta}.$$

The expressions of A and ϕ are given in terms of the state of the system (angle β_1 and β_2). We can insert these in the equations for how β_1 and β_2 evolve as a function of A and ϕ to get explicit expressions of β_1 , β_2 , ϕ and A as a function of time. This gives us the amplitude and phase of the optimal rf pulse as a function of time.